

# Glassy carbon electrode modified by Poly(m-aminobenzoic acid)/ nano SiO<sub>2</sub> film and electrical and electrochemical properties

Meysam Sharifirad<sup>1</sup>, Farhoush Kiani<sup>2</sup>, Fardad Koohyar<sup>2</sup>

<sup>1</sup>Department of Chemistry, Teacher research Bojnord, Iran; <sup>2</sup>Faculty of Science, Islamic Azad University, Ayatollah Amoli Branch, Amol, Iran

Received for publication: 15 March 2013.

Accepted for publication: 21 June 2013.

## Abstract

Poly(m-aminobenzoic acid) (m-ABA) film is deposited on glassy-carbon electrode (GCE) by electropolymerization in pH 7.0 phosphate buffer solutions (PBS). The electrochemical behavior of polymer film obtained is characterized by cyclic voltammetry (CV), electrochemical impedance spectroscopy (EIS), fourier transform infrared spectroscopy (FT-IR) and scanning electron microscopy (SEM) studies. In the present study, the effect of the scan rate on the current peak is investigated in the range of 50-200 mV/sec and, it is observed that the anodic and cathodic peak all increased with the solution pH until it reached 8 and then decreased until 11. In addition, a new electrode is developing by electrodeposition of SiO<sub>2</sub> nanoparticles on glassy-carbon electrode. The electrochemical behavior of polymer at the nanoparticles SiO<sub>2</sub>/GCE is investigated. Electrical properties as a function of frequency and temperature have also indicated a great interaction between epoxy matrix and different poly (m-aminobenzoic acid) / nano SiO<sub>2</sub> by physical mixing procedure.

**Keywords:** Aminobenzoic acid, electropolymerization, situ FT-IR spectroscopy, scanning electron microscopy, electrochemical impedance spectroscopy, SiO<sub>2</sub> nanoparticles.

## Introduction

Chemical modified electrodes (CMEs) become a field of exiting research due to their unique elec-

trode surfaces properties (Cheng *et al.*, 2005). Many techniques were developed for preparation of modified electrodes, such as covalent bonding and polymer film (Daum, & Murry, 1981). Deposit a film of conducting polymer was essential to work in a medium with an electrolyte that can protect the electrode surface from dissolution without impeding the electropolymerization process (Sharifirad *et al.*, 2010). Polymeric films possess three-dimensional extensity, a large number of reactive sites, good stability and offer the possibility to be designed with particular redox active sites (Dong *et al.*, 1995). Electropolymerization is a good approach to immobilize polymer as adjusting the electrochemical parameters can control film thickness, permission and charge transport characteristics (Kaya, & Aydin, 2010). Numerous monomers, such as, thiophene, pyrrole, anilin (Benyoucef *et al.*, 2009; Dalmolin *et al.*, 2005), p-aminobenzoic acid (Zhang *et al.*, 2010) and etc (Tanguy, 2000) were synthesized electrochemically and deposited onto different metal electrodes such as gold (Benyouce *et al.*, 2008), copper (Sharifirad *et al.*, 2010), aluminium and etc. monomer-containing electrolytes (Rudge *et al.*, 1994).

Hillman and coworkers (Hillman, & Mallen, 1987; Hillman, & Swann, 1988) suggested a deposition mechanism including instantaneous nucleation, followed by 3D growth of the nuclei until they overlap, leading to formation of a plain polymer layer. Different measurement techniques were applied to study the electrochemical polymerization of m-aminobenzoic acid (Cheng *et al.*, 2005) and

**Corresponding author:** Fardad Koohyar, Faculty of Science, Islamic Azad University, Ayatollah Amoli Branch, Amol, Iran. E-mail: FardadKoohyar@yahoo.com.

its derivatives. Most investigations were performed under potentiostatic control using potential pulse and potential sweep techniques. A number of other measurement techniques, such as, conductivity measurements, UV-vis spectroscopy (Hillman, & Swann, 1988) and also electrochemical impedance spectra (Sundfors & Bobacka, 2004) were applied recently. Electrochemical impedance spectroscopy was widely used for kinetic studies of electroactive polymer films, including both redox and conducting polymers

As well as there are several investigations performed to observe the effect of various parameters such as solvent (Yao *et al.*, 2007), electrolyte and temperature on the mechanical strength, stability, nanoparticle and conductivity (Sayyah *et al.*, 2008). In recent years, metal nanoparticles were attached much more attention in electroanalysis because of their unusual physical and chemical properties (Guo & Wang, 2011; Haldorai *et al.*, 2009; Liu *et al.*, 2010). Many nanomaterials including TiO<sub>2</sub> nanostructured films (Curulli *et al.*, 2005), carbon nanotubes (Wang & Musameh, 2003; Tsai *et al.*, 2007; Zhang & Gorski, 2005; Zhai *et al.*, 2006; Wu *et al.*, 2007a), carbon nanofibers (Wu *et al.*, 2007b; Wu *et al.*, 2008), mesoporous carbon (Wang *et al.*, 2009) and gold nanoparticles (Jena & Raj, 2006) were employed to improve the surface electrode. The sol-gel method (Li *et al.*, 1999) was one of the common techniques for preparing silicate films, superfine powders, composite materials, fibers and so on. This methodology provides a cryochemical approach to both designing and controlling the microstructure of materials. Metal nanoparticles, especially noble metal nanoparticles modified electrodes usually exhibit high electrocatalytic activities towards the compounds which have sluggish redox process at bare electrodes. As the most stable noble metal nanoparticles, gold nanoparticles (GNPs) were used increasingly in many electrochemical applications since they had the ability to enhance the electrode conductivity and facilitate the electron transfer, thus, improving the analytical performance (Sayyah *et al.*, 2008).

In the present work, m-aminobenzoic acid was selected as monomer for performing electrochemical polymerization in phosphate buffer solution. Cyclic voltammetry was used to deposit polymeric films on GC electrode as working electrode. m-Aminobenzoic acid (m-ABA) contains electron-rich N atom and high electron density of carbonyl

group, and it is easy to be polymerized on glassy-carbon electrode by CV. Jin and co-workers were applied poly (m-ABA) modified electrode to investigate an experimental parkinsonian animal model (Xu *et al.*, 2001). We investigate the scan rate, pH, conductivity and mechanism of electrochemical polymerization of m-aminobenzoic acid and m-aminobenzoic acid/SiO<sub>2</sub> in PBS solution on GC electrode. Also, the characterization of the obtained polymer films by IR, EIP and SEM were performed.

## Materials and methods

### Materials

m-Aminobenzoic acid (Fluka AG, Buchs SG, Switzerland) as the monomer, nano/SiO<sub>2</sub> (Allderich, Germany) and phosphate buffer solutions (PBS) with pH 7.0 as electrolyte that prepared by 0.1M NaH<sub>2</sub>PO<sub>4</sub>-Na<sub>2</sub>HPO<sub>4</sub> and adjusting the pH with 0.1M HCl and 0.1M NaOH.

### Apparatus

Cyclic voltammetry (CV) was carried out using a Potentiostat/Galvanostat EG&G Model 263 A; USA with a PC and electrochemical set up that controlled with M 270 software. Electrochemical impedance spectroscopy (EIS) was performed with a Frequency Response Detector EG&G Model 1025; USA with a PC and electrochemical set up that was controlled with M398 software. The FT-IR transmission spectrum of m-ABA coating was recorded in horizontally attenuated total reflectance mode in the spectral range 3500–550 cm<sup>-1</sup> using a Bruker spectrometer, Vector Series 22, Germany. Scanning electron microscopy (SEM) images were taken using a VEGA HV (high potential) 1500 V at various magnifications.

### Cell and Electrode

A conventional three-electrode system was employed with a bare or poly(m-ABA) modified glassy-carbon electrode (GCE) (1.0 mm diameter) as the working electrode, a Ag/AgCl (KCl: 3 M) electrode as the reference electrode and a platinum electrode as the counter electrode. Before each electrochemical experiment, the working electrode was mechanically polished with abrasive paper (2400 grade), then all of electrodes rinsed with distilled water and finally dried under argon flow. After deposition the working electrode was removed from the electrolyte and rinsed with double distilled water and then dried in air. All the measurements were carried out at room temperature.

### Preparation of materials

The electropolymerization solution consisting  $1.0 \times 10^{-3}$  M m-ABA was added to phosphate buffer as electrolyte solution. The electrochemical studies were performed at room temperature using the potentiodynamic polarization technique in the buffer solutions. The electrode was disposed by cyclic sweeping from -1.5 to 2.5 V at 50, 100, 150 and 200 mV/sec at 10, 20 and 50 circles in pH 7.0 PBS containing  $1.0 \times 10^{-3}$  M (m-ABA) solution. Then this work was repeat using nano  $\text{SiO}_2$  at same scan rates. The electrochemical impedance spectroscopy (EIS) measurements were performed in the presence of  $5.0 \times 10^{-3}$  M  $[\text{Fe}(\text{CN})_6]^{3-}/[\text{Fe}(\text{CN})_6]^{4-}$  as a redox probe.

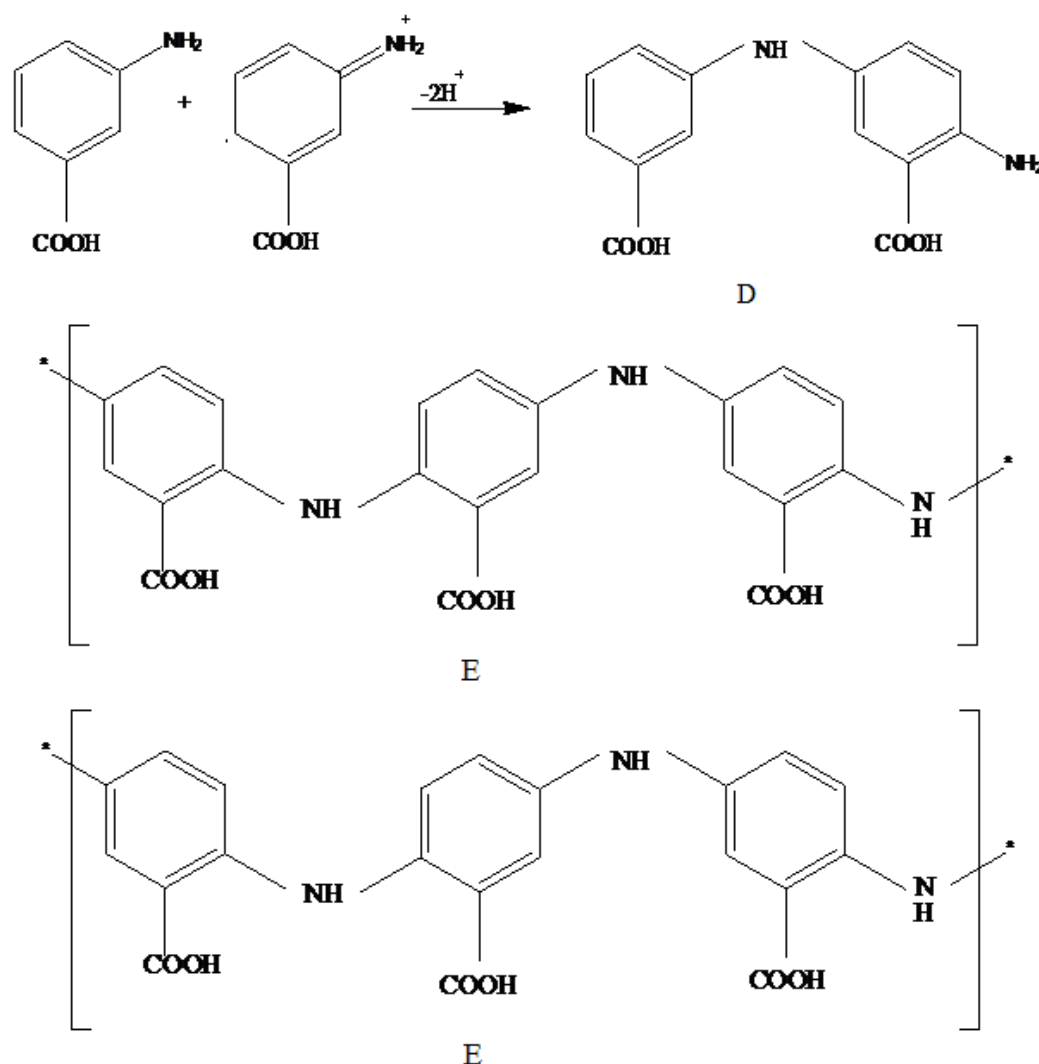
### Results and discussion

Electropolymerization of m-ABA on GCE surface  
Figure 1 shows the cyclic voltammograms (CVs) re-

corded during the oxidative polymerization of  $1.0 \times 10^{-3}$  M m-aminobenzoic acid in pH 7.0 phosphate buffer solution on GCE. In the first scan, anodic current peak 1 was observed with current value at  $180 \mu\text{A}$  and potential value at 1.66 V, respectively. Then, larger peak was observed upon continuous scanning, reflecting the continuous growth of the film. It can also be observed that film growth was faster for the first cycles than for the other cycles. From the seventh cycles, the film was hardly growth; the maximum of peak current was  $600 \mu\text{A}$ . It showed polymerization reached saturation. This fact indicated m-ABA was deposited on the surface of GCE by electropolymerization mode.

The mechanism of the electrochemical polymerization of monomer is believed to proceed via a radical cation which reacts with a second radical cation to give a dimer (Alishah and Holze, 2006)

In case of polymerization, the mechanism may be described as the follows Scheme 1.



Scheme 1. Oxidative polymerization of m-aminobenzoic acid.

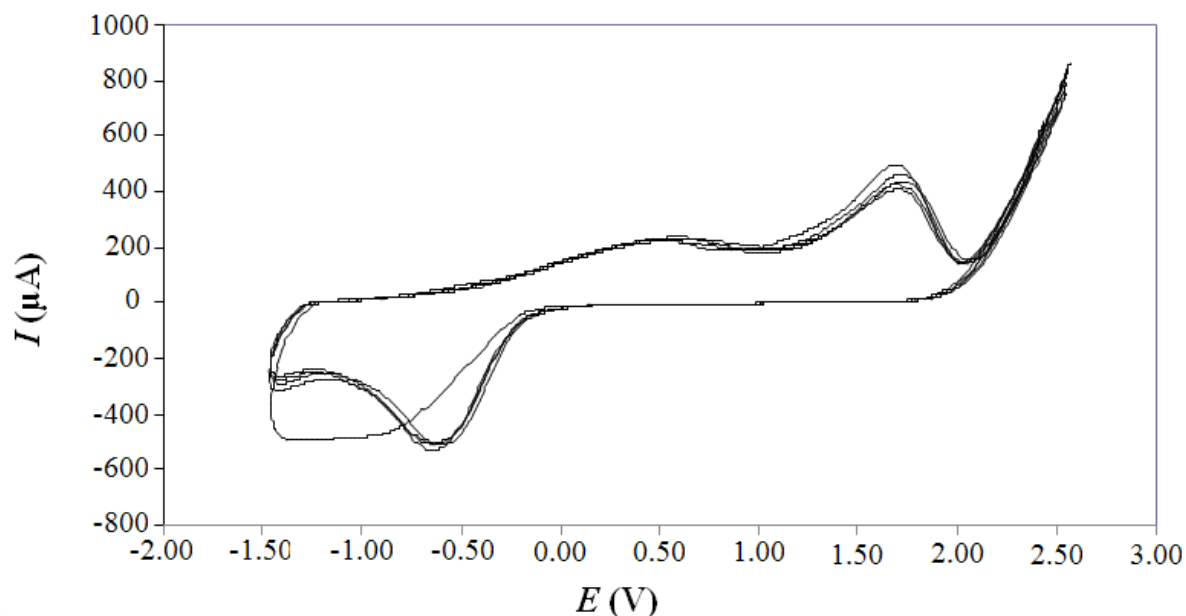


**Figure 1.** Cyclic voltammograms of  $1.0 \times 10^{-3}$  M m-ABA in pH 7.0 PB solution. Terminal potential, 2.5 V, potential, -1.5 V; scan rate, 100 mV/sec, for 50 cycles at the GC electrode.

It seems accepted that the first step involves the formation of a radical cation (Bard and Yang, 1992). Later, this intermediate forms a dimeric species by para-coupling with either an unoxidized monomer or another radical cation giving rise to the propagation of the reaction. This mechanism (involving para-coupling) is assumed to be valid also for the oxidative polymerization of m-aminobenzoic acid, as it has been illustrated in Scheme 1. It will be shown below that in FT-IR spectroscopy results are also compatible with the polymer structure derived from this kind of mechanism.

#### *Effect of the solution pH on the anodic current peak*

The effect of solution pH on the formation of polymeric film was investigated over the range

of 3-11. Anodic and cathodic current peak all increased with the solution pH until it reached 8 and then decreased until pH reached 11. Figure 2 shows that the cathodic current peak changed with increasing pH (Table 1).

#### *Effect of increasing scan rate on the anodic current peak*

The effect of increasing scan rate on the current peak was investigated in the range of 50-200 mV/sec. The anodic current peak was proportional to the scan rate (Figure 3). This result shows that the current peak shifted to the positive direction at higher scan rates because when scan rate was increased, the monomers were received sooner to the electrode surface, similarly, the current increased (Table 2).

**Table 1.** The values of the anodic current on GC/m-ABA electrode with different pH.

pH	5	6	7	8	9	10	11
Anodic current (mA)	0.34	0.47	0.48	0.56	0.56	0.54	0.51

**Table 2.** The values of the anodic current on GC/m-ABA electrode with different scan rate.

Scan rate (mV/sec)	50	100	150	200
Anodic current (mA)	0.445	0.452	0.471	0.478

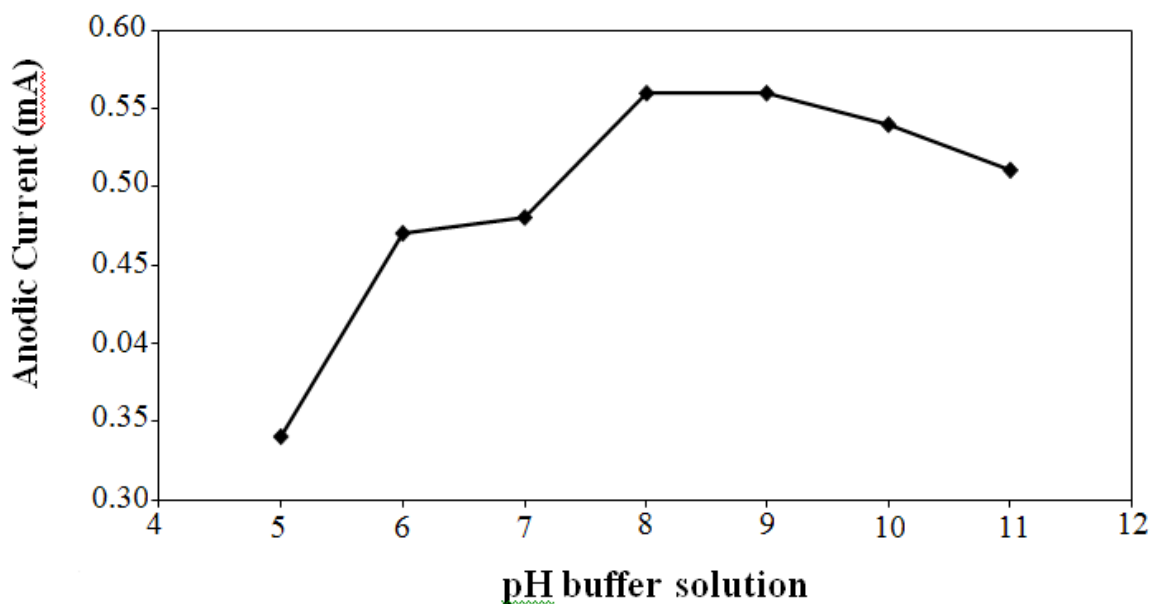


Figure 2. The effect of pH on the anodic current peak; scan rate, 100 mV/sec.

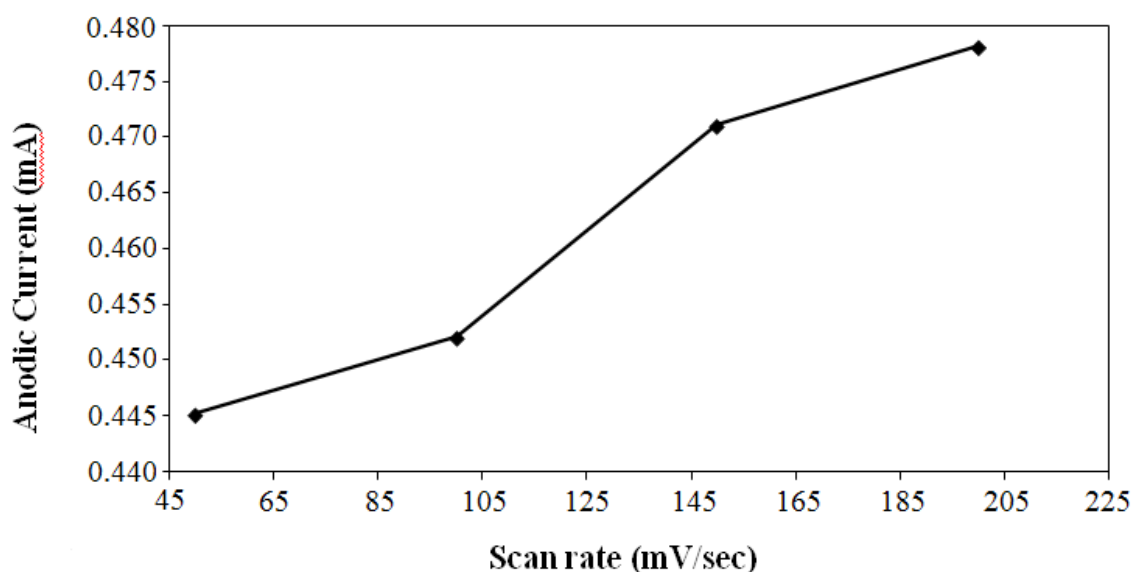


Figure 3. Effect of increasing scan rate on the anodic current peak.

#### *Electrochemical impedance characterization of poly (m-ABA) modified electrode*

As is well known from measurements performed under potential control, the low frequency impedance of the polymer covered electrodes can be approximated by a limiting low frequency capacitance and a series resistance (Popkirov and Barsoukov, 1995; Popkirov *et al.*, 1997).

The EIS experiments were carried out in  $5.0 \times 10^{-3}$  M  $[\text{Fe}(\text{CN})_6]^{3-}/[\text{Fe}(\text{CN})_6]^{4-}$  solution. Figure 4 shows

the plots ( $Z''$  vs.  $Z'$ , Nyquist plot) of the EIS obtained at the modified GC electrode and at the modified GC electrode with nanoparticles. The results indicated that the electron-transfer resistance of polymer film was increased with the increase of the  $\text{SiO}_2$  adsorption on electrode and conductivity was decreased. By these results qualitative characteristics of electron-transfer resistance of the modified electrode were determined (Wang *et al.*, 2004).

### Spectroscopic characterization of the produced poly (*m*-ABA) film

The FT-IR spectrum of the film produced in PB solution was deposited in Figure 1. A band at  $\sim 3300\text{--}3450\text{ cm}^{-1}$  was due to the characteristic N–H stretching vibration. The band at  $\sim 3400\text{ cm}^{-1}$  was assigned to O–H stretching mode in carboxylic

acid. Also a band observed at  $\sim 1500\text{ cm}^{-1}$  was due to carbonyl group at in carboxylic acid. In addition, a band appearing at  $1100\text{ cm}^{-1}$  related to the single band aromatic C–N stretching in secondary aromatic amines. The electropolymerization mechanism can be easily proposed by this band (Figure 5).

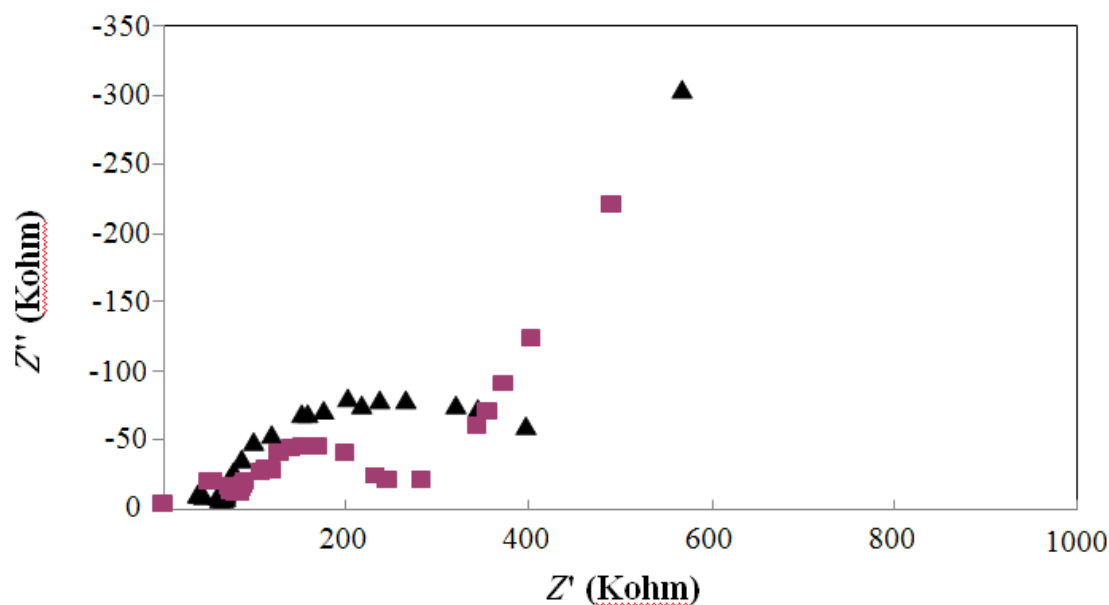


Figure 4. The inquest impedance plots for (a) modified electrode, (b) modified electrode with nanoparticles of  $\text{SiO}_2$ .

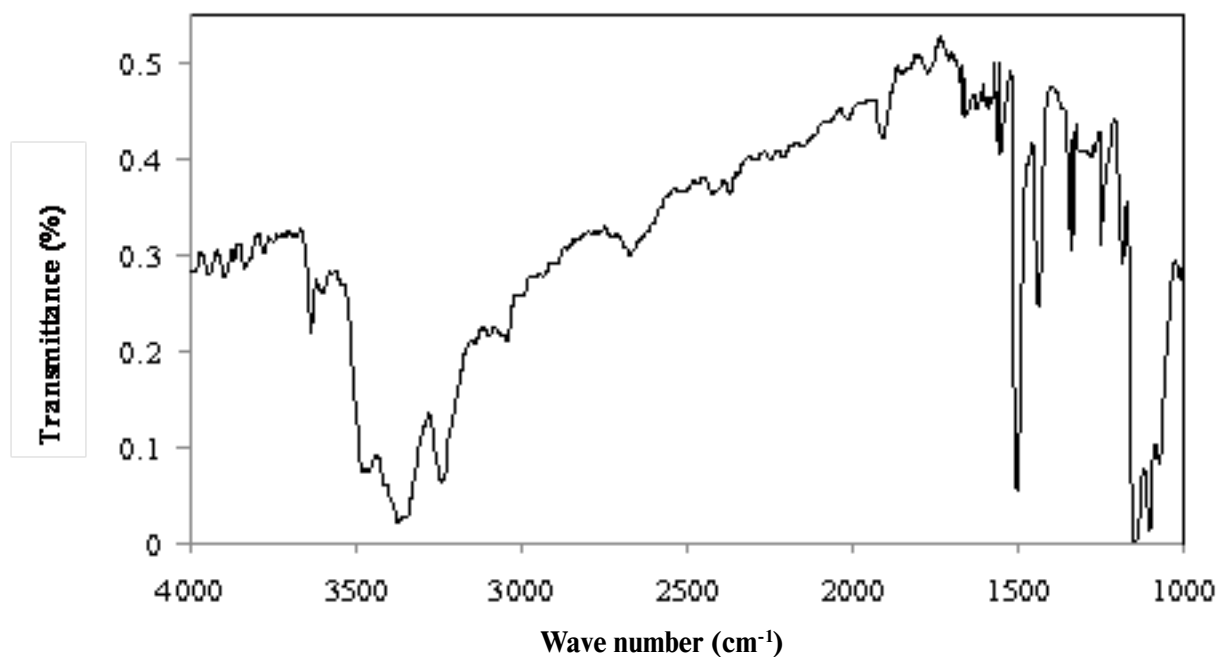
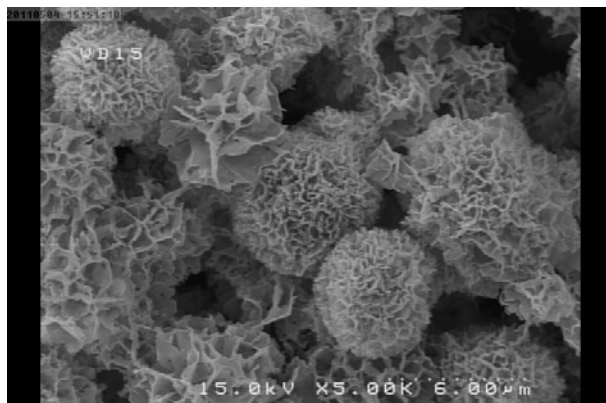


Figure 5. FT-IR spectrum of the poly *m*-aminobenzoic acid coating synthesized on GC substrate under cyclic voltammetric condition

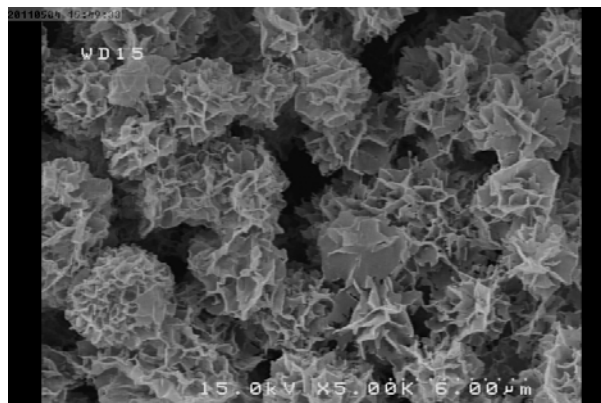
### Surface analysis of deposited poly(*m*-ABA)

The SEM images of the electrodeposited poly(*m*-ABA) film and poly(*m*-ABA) using SiO<sub>2</sub> are shown in Figure 6. The polymer is formed by cyclic voltammetry

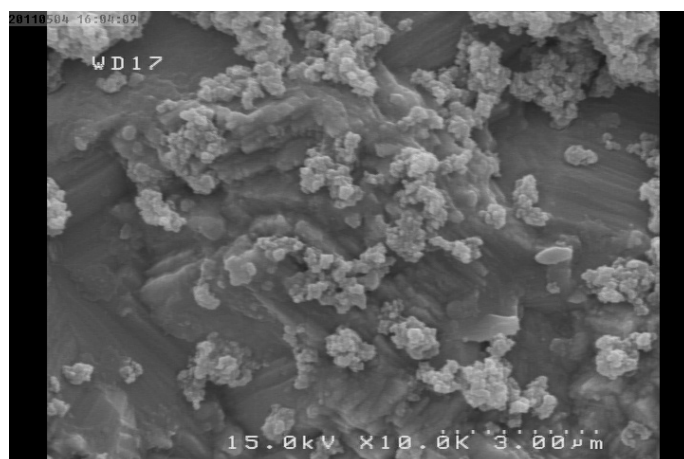
mode for 25 cycles. In Figure 6 (a,b), poly(*m*-ABA) film appears thin on the carbon electrode. In the case of sodium acetate solution, Figure 6c, the film morphology is more granular and the film reaches a higher thickness.



a)



b)



c)

**Figure 6.** SEM images of polymer coated GCE: (a,b) *m*-ABA, (c) *m*-ABA SiO<sub>2</sub>.

### Effect of using nanoparticles of SiO<sub>2</sub> on the formation of poly(*m*-ABA)

Figure 7 show the cyclic voltammograms (CVs) recorded during the oxidative polymerization of  $1.0 \times 10^{-3}$  M *m*-aminobenzoic acid by using nano SiO<sub>2</sub> in pH 7.0 phosphate buffer solutions on GCE. In the first scan, anodic current peak 1 was observed with current value at 132  $\mu$ A and potential value at 1.55 V, respectively. Then, larger peak were observed upon continuous scanning, reflecting the continuous growth of the film. This fact indicated poly *m*-ABA/nano SiO<sub>2</sub> was deposited on the surface of GCE by electropolymerization mode. It can be observed that currents of

all peaks in the synthesis of films increased quickly with the number of cycles and also their peak currents were lower than those of the corresponding peaks in Figure 1 at the same cycle, the maximum of current peak was 520  $\mu$ A thus, it is interesting to note that the board voltammetric charge decrease by the increase of the amount of nano SiO<sub>2</sub> for mixture of the monomers.

Figure 8 shows CVs of *m*-ABA and *m*-ABA/SiO<sub>2</sub> modified electrode, at both of them, compared of current peak can be investigated for fiftieth cycles. The results indicated that the conductivity of polymer film was decreased with the increase of the nano SiO<sub>2</sub> adsorption on electrode.

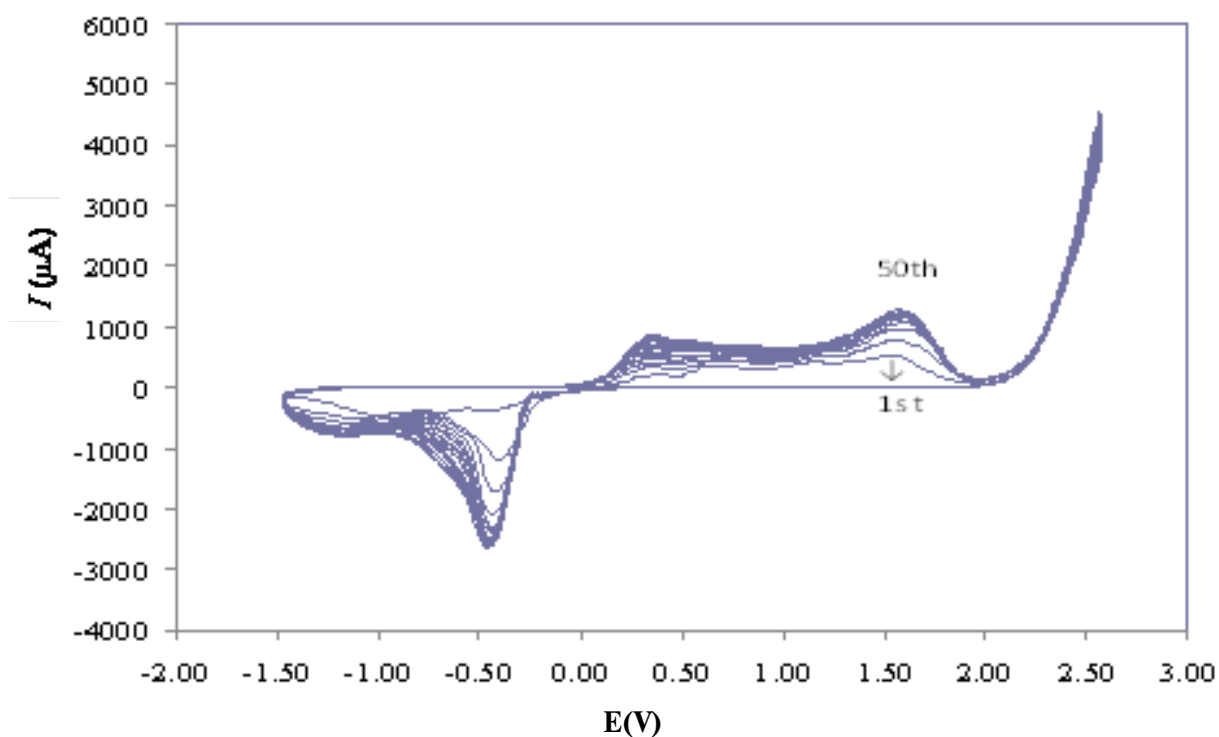


Figure 7. Cyclic voltammograms of  $1.0 \times 10^{-3}$  M m-ABA by using SiO<sub>2</sub> in pH 7.0 PB solution. Terminal potential, 2.5 V, potential, -1.5 V; scan rate, 100 mV/sec, for 50 cycles at the GC electrode.

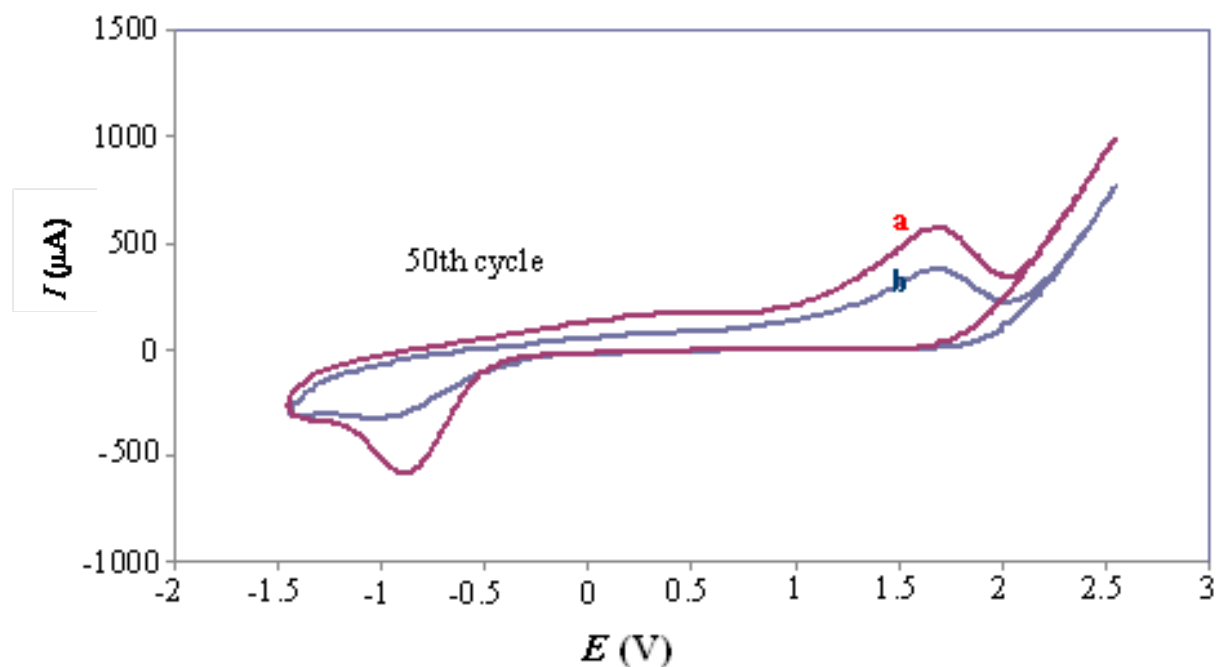


Figure 8. Cyclic voltammograms on a GC electrode (1 cycle): (a) m- ABA, (b) m-ABA/SiO<sub>2</sub>.

*Effect of the scan rate on the formation of poly(m-ABA) using nanoparticles SiO<sub>2</sub>*

The effect of increasing scan rate on the anod-

ic current peak was investigated in the range of 50-200 mV/sec. The result shows that the anodic current peak shifted to the positive direction at higher

scan rates until scan rate reached 150 mV/sec and then decreased until it reached 200 mV/sec. These results indicated that maximum of current observed at the 150 mV/sec, because when the scan rate increased more than 150 mV/sec pieces of electroactive did not have enough time to receive to the

electrode surface, therefore the faradic current decreased (Table 4, Figure 9). Also the values of the impedance parameters from the fit to the equivalent circuit for the impedance spectra recorded for GC/m-ABA and GC/m-ABA/nano SiO<sub>2</sub> electrode are listed in Table 3.

**Table 3.** The values of the impedance parameters from the fit to the equivalent circuit for the impedance spectra recorded for GC/m-ABA and GC/m-ABA/SiO<sub>2</sub> electrode.

Sample	Rct (Ω/cm <sup>2</sup> )	Rcd (Ω/cm <sup>2</sup> )	Rsol (Ω/cm <sup>2</sup> )
GCE/m-ABA	49.6	179.4	64.2
GCE/m-ABA/SiO <sub>2</sub>	68.2	275.1	68.3

**Table 4.** The values of the anodic current in Fig. 9 for GC/m-ABA/SiO<sub>2</sub> electrode with different scan rate

Scan rate (mV/sec)	50	100	150	200
Anodic current (mA)	0.345	0.425	0.556	0.365

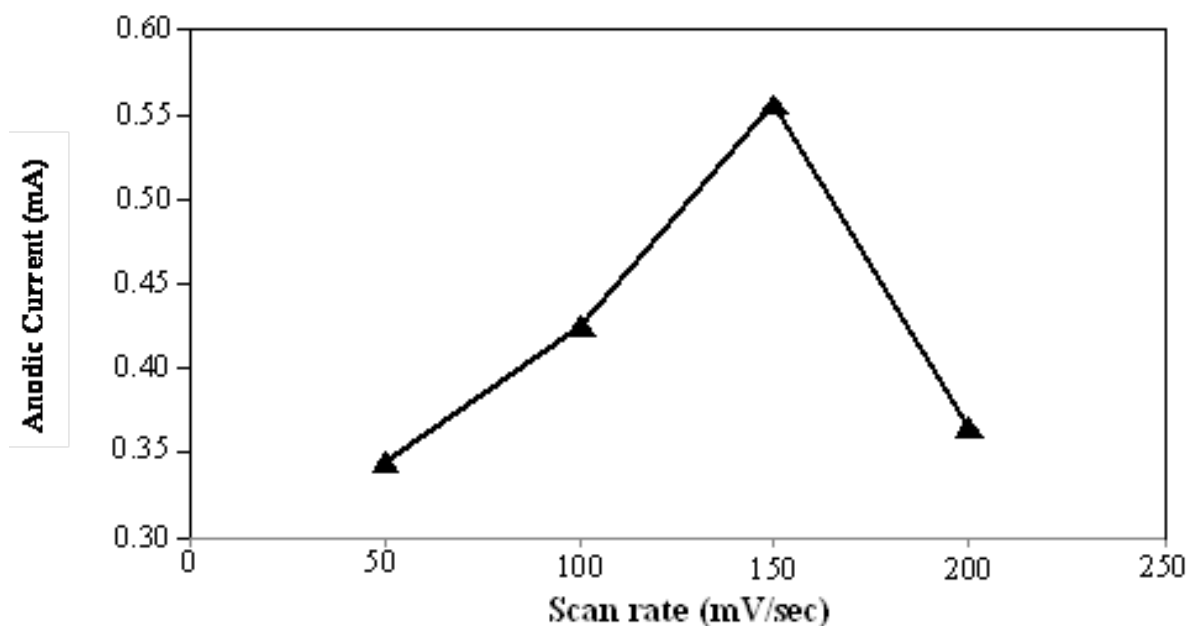


**Figure 9.** Effect of increasing scan rate on the anodic current peak by using SiO<sub>2</sub>.

#### *XRD Studies of poly (m-aminobenzoic acid) / SiO<sub>2</sub>*

Figure 10 shows the XRD patterns of the pure poly (m-aminobenzoic acid) and its nanocomposites reinforced with poly (m-aminobenzoic acid) / SiO<sub>2</sub> nanocomposite loadings. The peaks at 17.5°

and 40.0° were observed in the pure poly (m-aminobenzoic acid). The first peak has a d-spacing of 0.454 nm, corresponding to the typical doublet reflection of the planes of the semi crystalline atactic poly (m-aminobenzoic acid). The second peak is

assigned to the plane of the poly (m-aminobenzoic acid). The peak corresponding to the plane of the poly (m-aminobenzoic acid) becomes narrower and narrower as a function of the particle loading. The average particle size (L) was estimated from the Debye–Scherrer equation.

$$L = \frac{K\lambda}{\beta(2\theta)\cos\theta} \quad (1)$$

Where  $\beta(2\theta)$  is the full width at half-maximum (FWHM), K is a constant taken as the normal value of 0.9,  $\lambda$  is the wavelength of X-ray wavelength (for copper,  $K = 1.5406 \text{ \AA}$ ), and L is the Bragg angle. The crystal plane at  $2\theta = 23.5^\circ$  was used to estimate the particle size. The calculated values are about 15 to 20 nm for poly (m-aminobenzoic acid).

This suggests a higher crystallinity of the poly (m-aminobenzoic acid), which is in contrast to  $\text{SiO}_2$  nanocomposites reinforced with poly (m-aminobenzoic acid). The presence of  $\text{SiO}_2$  nanocomposites favors the recrystallization of poly (m-aminobenzoic acid) during the polymer solution

solidification process. Concurrently, the standard  $\text{SiO}_2$  nanocomposites reflection peaks are observed, similar to Figure 10.

### Electrical Conductivity Studies of poly (m-aminobenzoic acid) / $\text{SiO}_2$

Figure 11 displays the conductivities of the poly (m-aminobenzoic acid) /  $\text{SiO}_2$  samples prepared using both the absorption-transferring and blending processes. As shown in Figure 11, the conductivity of the hybrid prepared using the absorption-transferring process was higher than that from the blending process regardless of the content of poly (m-aminobenzoic acid) /  $\text{SiO}_2$ . In addition, the percolation threshold was also lower because the DDS molarity aggregated readily during the latter process. In the absorption-transferring process, when the content of poly (m-aminobenzoic acid) /  $\text{SiO}_2$  reached a threshold, the conductivity of the hybrid increased thereafter because the poly (m-aminobenzoic acid) /  $\text{SiO}_2$  composite aggregated into secondary particles. Not only did this process cause the poly (m-aminobenzoic acid) /  $\text{SiO}_2$  chains to entangle readily, it also interrupted the conducting pathway.

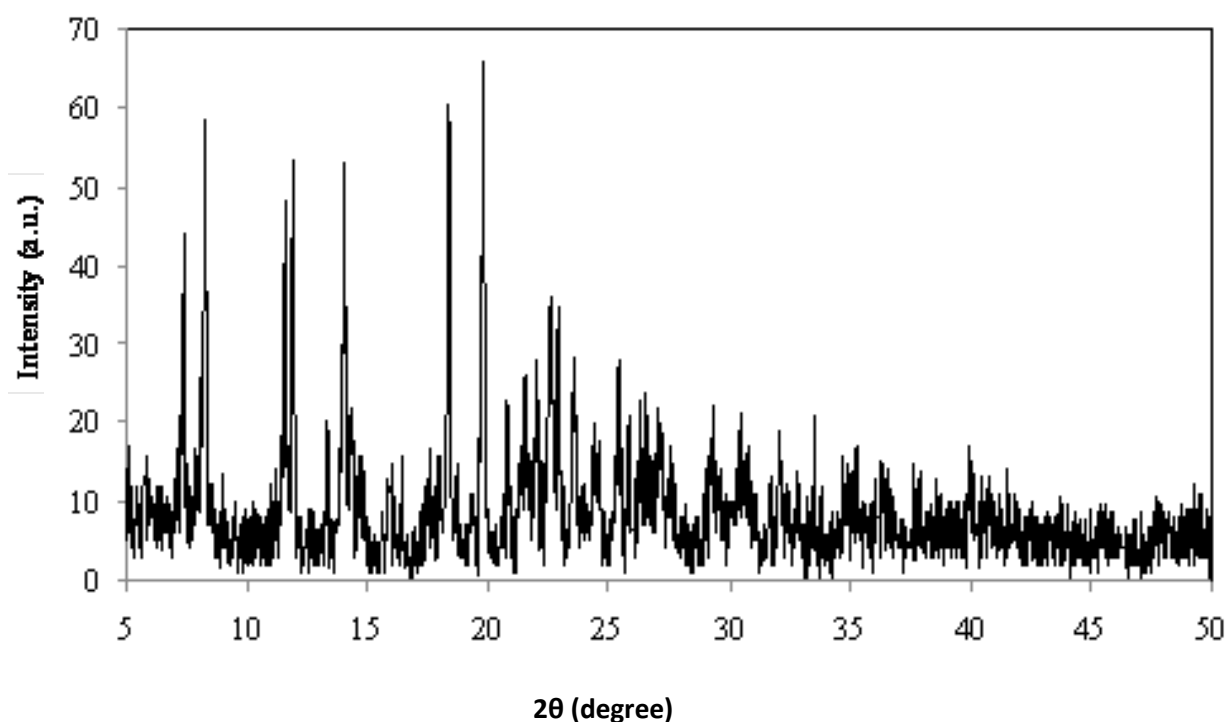


**Figure 10.** X-ray diffraction patterns of (poly (m-aminobenzoic acid) /  $\text{SiO}_2$ ).

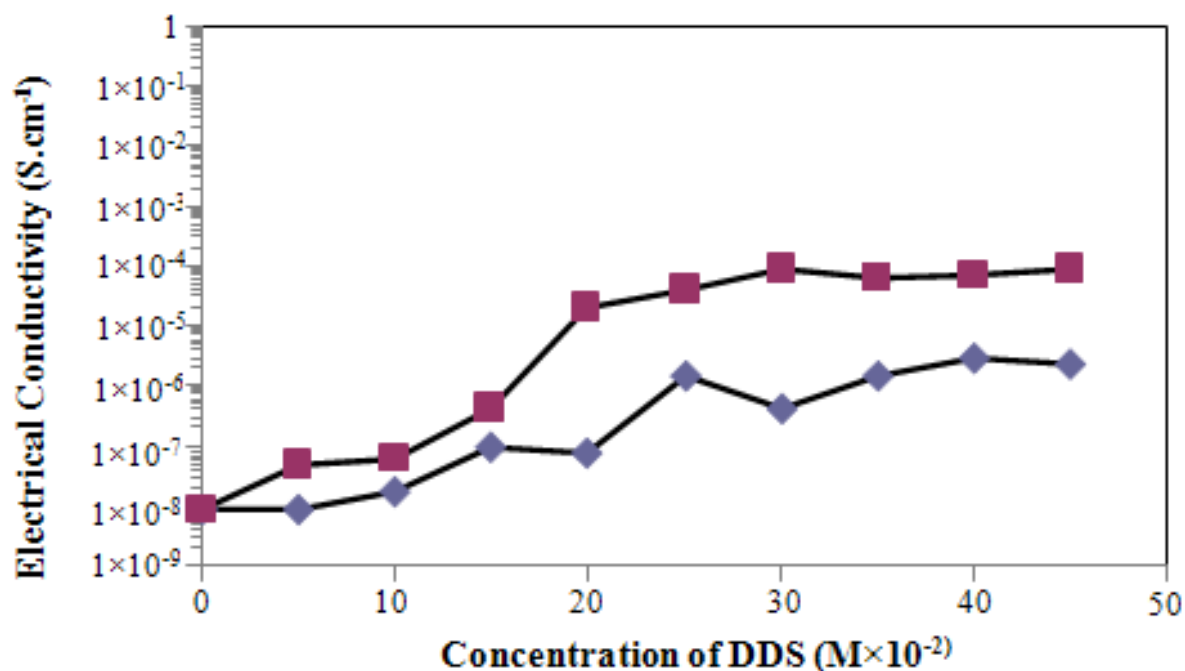


Figure 11. Electrical conductivity of (a) poly (m-aminobenzoic acid) (b) poly (m-aminobenzoic acid) / SiO<sub>2</sub>.

## Conclusions

Poly(m-aminobenzoic acid) was deposited on a glassy-carbon electrode to form film modified electrode. Also the SiO<sub>2</sub> nanoparticles were electrochemically generated on the glassy-carbon electrode surface. In addition, the effect of solution pH on the current response was investigated. Anodic and cathodic current peak all increased with the solution pH until it reached 8. FT-IR spectroscopy technique allowed obtaining the para-coupling mechanism. According to cyclic voltammetry, composite poly (M-amino benzoic acid) / nano SiO<sub>2</sub> (silica) anodic peak current on the scan rate is 150 mV/s. EIS studies were indicated that the electron-transfer resistance of polymer film was increased with the increase of the SiO<sub>2</sub> adsorption on electrode. The X-ray spectra showed that the size of the particles in the composite structure is approximately between 15 and 20 nm. Also, SEM images demonstrate the nanoparticles of composites. In the other hand, the anodic current for the composite poly (m-aminobenzoic acid) is more than other poly (M-amino benzoic acid) /nano SiO<sub>2</sub> (silica), respectively.

## References

- Alishah A. H., & Holze R. 2006. Poly(o-aminophenol) with two redox processes: a spectroelectrochemical study. *J. Electroanalytical. Chem*, 597: 95-102
- Bard J and Yang H., 1992. The application of fast scan cyclic voltammetry. Mechanistic study of the initial stage of electropolymerization of aniline in aqueous solutions. *J. Electroanalytical. Chem*, 239: 423-449
- Benyouce A., Huerta F., Errahi M. I. & Morallon E., 2008. Voltammetric and in situ FT-IRS study of the electropolymerization of O-aminobenzoic acid at gold and graphite carbon electrodes: influence of pH on the electrochemical behaviors of polymer films. *J. Electroanalytical. Chem*, 624: 245-250
- Benyoucef A., Boussalem S, & Belbachir M., 2009. Electrochemical synthesis of poly(o-aminobenzoic acid) and poly(o-aminobenzoic acid-co-aniline): electrochemical and in-situ FTIRS characterization. *World. J. Chem*, 4: 171-177
- Cheng W., Jin G. & Zhang Y., 2005. Electrochemical characteristics of poly(o-aminobenzoic acid) modified glassy-carbon electrode and its electro-

- catalytic activity towards oxidation of epinephrine. *Russian. J. Electrochem*, 41: 940-945
- Curulli A., Valentini E., Padeletti G., Viticoli A., Caschera D & Palleschi G., 2005. Smart (nano) materials: TiO<sub>2</sub> nanostructured films to modify electrodes for assembling of new electrochemical probes. *Sens. Actuator, B: chemistry*, 111: 441-449
- Dalmolin C., Canobre S.C., Biaggio S.R., Rocha-Filho R. & Bocchi N., 2005. Electropolymerization of polyaniline on high surface area carbon substrates. *J. Electroanalytical. Chem*, 578: 9-15
- Daum P., & Murry R.W., 1981. Charge-transfer diffusion rates & activity relationships during oxidation and reduction of plasma-polymerized vinylferrocene films. *J. Physical. Chem*, 85:389-396
- Dong S.J., Che G.L. & Xie Y.W., 1995. Chemically modified electrode. Chinese Science Press. Beijing, p: 39.
- Guo S., & Wang E., 2011. Noble metal nanomaterials: Controllable synthesis and application in fuel cells and analytical sensors. *Nano Today*, 6: 240-264
- Haldorai Y., Long P.Q., Noh S.K., Lyoo W.S. & Shim J.J., 2009. *Polymer Advance Technology*, Wiley & Sons, Ltd.
- Hillman A.R., & Mallen E.F., 1987. Nucleation and growth of polythiophene films on gold electrodes. *J. Electroanalytical. Chem*, 220: 351-367
- Hillman A.R., & Swann M.J., 1988. Spectroscopic studies of the growth and potential cycling of polybithiophene films. *Electrochimical Acta*, 33: 1303-1312
- Huang S.W., Neoh K.G., Kang E.T., & Tan K.L., 1998. Palladium-containing polyaniline and polypyrrole microparticles. *J. Mater Chem*, 8: 1743-1748
- Jena B.K., & Raj C.R., 2006. Electrochemical biosensor based on integrated assembly of dehydrogenase enzymes and gold nanoparticles. *Anal. Chem*, 78 : 6332-6339
- Kaya I., & Aydin A., 2010. Synthesis, characterization, thermal stability, conductivity, and band gaps of substitute oligo/polyamines or polyphe-nol. *Polymers. Adv. Technol*, 21: 337-347
- Li J., Chia L.S., Goh N.K. & Tan S.N., 1999. Renewable silica sol-gel derived carbon composite based glucose biosensor. *J. Electroanalytical. Chem*, 460: 234-241
- Liu X., Li B., Wang X & Li C., 2010. One-step construction of an electrode modified with electro-deposited Au/SiO<sub>2</sub> nanoparticles, and its application to the determination of NADH and ethanol. *Microchimical Acta*, 171: 399-405
- Lu X., Yu Y., Chen L., Mao H., Zhang W & Wei Y., 2004. Preparation and characterization of polyaniline microwires containing CdS nanoparticles, *Chem. Commun*, 13: 1522-1523
- Popkurov G.S & Barsoukov E., 1995. In-situ impedance measurements during oxidation and reduction of conducting polymers: significance of the capacitive currents. *J. Electroanalytical. Chem*, 383: 155-160
- Popkurov G.S., Barsoukov E & Schindler R.N., 1997. Investigation of conducting polymer electrodes by impedance spectroscopy during electropolymerization under galvanostatic conditions. *J. Electroanalytical. Chem*, 425, 209-216
- Rudge A., Raistrick J., Gottesfeld S. & Ferraris P., 1994. A study of the electrochemical properties of conducting polymers for application in electrochemical capacitors. *Electrochimical Acta*, 39:273-287
- Sayyah S.M., El-Rabiey M.M., El-Rehim S.S.A & Azooz R.E., 2008. Electropolymerization kinetics of a binary mixture of pyrrole and O-aminobenzoic acid and characterization of the obtained polymer films. *J. Appl. Polymer. Sci*, 109:1643-1653
- Sharifirad M., Omrani A., Rostami A.A. & Khoshroo M., 2010. Electrodeposition and characterization of polypyrrole films on copper. *J. Electroanalytical. Chem*, 645: 149-158
- Stejskal J., Trchova M., Prokes J. & Sapurina I., 2001. Brominated Polyaniline, *Chem. Mater*, 13: 4083-4086
- Sundfors F. & Bobacka J., 2004. EIS study of the redox reaction of Fe(CN)<sub>6</sub><sup>3-/4-</sup> at poly(3,4-ethylenedioxythiophene) electrodes: influence of DC potential and COX: CRed ratio. *Journal of Chemistry*, 572: 309-316
- Tanguy J., 2000. On the electropolymerization of methacrylonitrile and acrylonitrile as studied by CV, EQCM and EIS. *J. Electroanalytical. Chem*, 487: 120-132
- Tsai Y.G., Huang J.D. & Chiu C.C., 2007. Amperometric ethanol biosensor based on poly(vinyl alcohol)-multiwalled carbon nanotube-alcohol dehydrogenase biocomposite. *Biosens Bioelectron*, 22: 3051-3056
- Wang J., Fireston M.A., Auciello O. & Carlisle J.A., 2004. Surface functionalization of ultrananocrystalline diamond films by electrochemical reduction of aryldiazonium salts. *Langmuir*, 20:11450-11456

- Wang J. & Musameh M., 2003. Carbon nanotube/teflon composite electrochemical sensors and biosensors. *Anal. Chem*, 75: 2075-2079
- Wang Y., You C.P., Zhang S., Kong J.L., Marty J.L., Zhao D.Y & Liu B.H., 2009. Electrocatalytic oxidation of NADH at mesoporous carbon modified electrodes. *Microchimical Acta*, 167:75-79
- Wu B.Y., Hou S.H., Yin F., Zhao Z.X., Wang Y.Y., Wang X.S & Chen Q., 2007. Amperometric glucose biosensor based on multilayer films via layer-by-layer self-assembly of multi-wall carbon nanotubes, gold nanoparticles and glucose oxidase on the Pt electrode. *Biosens Bioelectron*, 22: 2854-2860
- Wu L., Zhang X & Ju H., 2007. Detection of NADH and ethanol based on catalytic activity of soluble carbon nanofiber with low overpotential. *Anal. Chem*, 79: 453-458
- Wu L., Lei J., Zhang X & Ju H., 2008. Biofunctional nanocomposite of carbon nanofiber with water-soluble porphyrin for highly sensitive ethanol biosensing. *Biosensors and Bioelectronics*, 24: 644-649
- Xu F., Gao M.N., Wang L., Shi G.Y., Zhang W., Jin L.T & Jin J.Y., 2001. Sensitive determination of dopamine on poly(aminobenzoic acid) modified electrode and the application toward an experimental parkinsonian animal mode. *Talanta*, 55: 329-336
- Yao H., Sun Y., Lin X., Tang Y & Huang L., 2007. Electrochemical characterization of poly(eriochrome black T) modified glassy carbon electrode and its application to simultaneous determination of dopamine, ascorbic acid and uric acid. *Electrochimical Acta*, 52: 6165-6171
- Zhai X.R., Wei W.Z., Zeng J.X., Gong S.J & Yin J., 2006. Layer-by-layer assembled film based on chitosan/carbon nanotubes, and its application to electrocatalytic oxidation of NADH. *Microchimical Acta*, 154: 315-320
- Zhang M.G & Gorski W., 2005. Electrochemical sensing platform based on the carbon nanotubes/redox mediators-biopolymer system. *J. American. Chem. Soc*, 127: 2058-2059
- Zhang Y., Wang J & Xu M., 2010. A sensitive DNA biosensor fabricated with gold nanoparticles/poly(P-aminobenzoic acid)/carbon nanotubes modified electrode. *Colloids and Surfaces B: Bio-interfaces*, 75: 179-185